FASTER-THAN-NYQUIST SIGNALING VIA SPATIOTEMPORAL SYMBOL-LEVEL PRECODING FOR MULTI-USER MISO REDUNDANT TRANSMISSIONS

Wallace Alves Martins,[⋆†] *Danilo Spano,*[⋆] *Symeon Chatzinotas,*[⋆] *Björn Ottersten*[⋆]

[⋆] Interdisciplinary Centre for Security Reliability and Trust (SnT), University of Luxembourg, Luxembourg
[†]DEL/Poli & PEE/COPPE, Federal University of Rio de Janeiro (UFRJ), Brazil

ABSTRACT

This paper tackles the problem of both multi-user and intersymbol interference stemming from co-channel users transmitting at a faster-than-Nyquist (FTN) rate in multi-antenna downlink transmissions. We propose a framework for redundant block-based symbol-level precoders enabling the trade-off between constructive and destructive multi-user and interblock interference (IBI) effects at the single-antenna user terminals. Redundant elements are added as guard interval to handle IBI destructive effects. It is shown that, within this framework, accelerating the transmissions via FTN signaling improves the error-free spectral efficiency, up to a certain acceleration factor beyond which the transmitted information cannot be perfectly recovered by linear filtering followed by sampling. Simulation results corroborate that the proposed spatiotemporal symbol-level precoding can change the amount of added redundancy from zero (full IBI) to half (IBI-free) the equivalent channel order, so as to achieve a target balance between spectral and energy efficiencies.

***Index Terms*—** Symbol-level precoding (SLP), faster-than-Nyquist (FTN) signaling, multi-user interference (MUI), interblock interference (IBI), multiple-input single-output (MISO)

1. INTRODUCTION

Symbol-level precoding (SLP) [1] accounts for the underlying multi-user interference (MUI) in full frequency-reuse downlink transmissions by shaping the transmitted waveforms so as to induce a constructive interference at each user [2, 3, 4]. SLP is a non-linear technique that uses channel-state information (CSI) along with users' data to form the precoder. Several SLP schemes exploiting different properties of the communication environment have been proposed [5, 6, 7, 8, 9]; a survey on SLP can be found in [10].

In addition to aggressive frequency reuse, faster-than-Nyquist (FTN) signaling [11] has recently been considered as a viable alternative for enhancing spectral efficiency by accelerating the transmission of symbols beyond the Nyquist limit [12, 13, 14, 15]. Although most FTN schemes focus on compensating the introduced intersymbol interference (ISI) at the receiver end, some recent works tackle the ISI using SLP-inspired techniques [16, 17, 18, 19].

While standard SLP schemes work only in the spatial domain to handle MUI, spatiotemporal SLP schemes [16] also deal with the FTN-related ISI by working in both spatial and temporal domains. Indeed, the spatiotemporal SLP splits the users' data in temporal blocks and jointly handles the ISI/MUI within each transmitted block. A key problem that spatiotemporal SLP schemes face is the inherent interblock interference (IBI), which has only been partially addressed by the so-called sequential spatiotemporal SLP [20, 21].

In this work we propose a framework for addressing the FTN-related IBI effects in spatiotemporal SLP schemes by adapting to the non-linear setup some well-known ideas from reduced-redundancy linear transceivers [22, 23, 24, 25, 26, 27]. The resulting spatiotemporal precoders allow for the trade-off between constructive and destructive IBI effects, and generalize the proposals from [20, 21].

The paper is organized as follows. A new multiple-input single-output (MISO) system model for SLP redundant transmissions is proposed in Section 2; a detailed study on FTN effects over the transmissions is conducted in Section 3, where we show the monotonicity of the error-free spectral efficiency with respect to the sampling time and the minimum admissible sampling time that allows for information losslessness; the specific way redundancy is added/removed as well as the minimum guard-interval length enabling IBI-free transmissions are described in Section 4; and the proposed spatiotemporal SLP is described in Section 5. All results are supported by numerical experiments in Section 6.

Notation: Scalars are denoted by italic letters, whereas vectors and matrices are denoted by boldface letters (lowercase for vectors and uppercase for matrices). Calligraphic letters denote sets. Discrete-time signals are expressed with brackets and continuous-time signals with parentheses; $\delta[n]$ is the Kronecker discrete-time pulse, whereas $\delta(t)$ is the Dirac continuous-time impulse. The Fourier transform of $f(t)$ is denoted as $F(\mathrm{j}\omega)$. The symbols $\triangleq$ and $*$ denote definition assignment and linear convolution, respectively. The notations $(\cdot)^{\mathrm{T}}$ and $(\cdot)^{\mathrm{H}}$ stand for transpose and Hermitian transpose operations on $(\cdot)$, respectively. Given a real number x, $\lfloor x \rfloor$ and $\lceil x \rceil$ respectively stand for the largest integer smaller than or equal to x and the smallest integer greater than or equal to x.

2. SYSTEM MODEL

Consider the base-band system model of a downlink transmission to K single-antenna user terminals via $N \geq K$ antennas, whose transmitter is illustrated in Fig. 1.

The model assumes perfect time-frequency synchronization and perfect CSI knowledge at the transmitter side. The system works in a block-based manner, so that the data stream to be delivered to the k^{th} user is divided into non-overlapping blocks with M symbols from a complex-valued constellation $\mathcal{C}$. Let $s_k[m] \in \mathcal{C}$, with $m \in \mathcal{M} \triangleq \{0, 1, \ldots, M-1\}$, denote the constellation symbols of one block to be transmitted to the k^{th} user, and $\boldsymbol{s}_k$ denote a vector gathering the M symbols of the block. All vectors $\boldsymbol{s}_k$, with $k \in \mathcal{K} \triangleq \{0, 1, \ldots, K-1\}$, are jointly processed to yield the pre-

The work is funded by the Luxembourg National Research Fund (FNR) through the projects: CI-PHY, ECLECTIC, and PROSAT. The work was also financed in part by FAPERJ (Brazil).

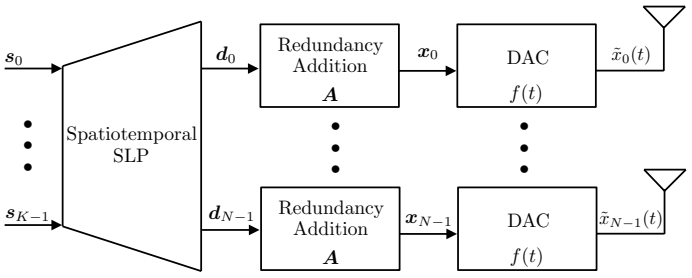

Fig. 1. Multi-user MISO base-band transmitter.

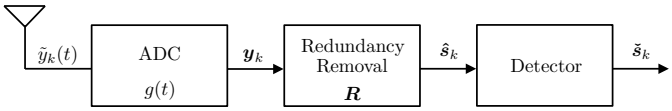

Fig. 2. Single-antenna base-band receiver.

coded vectors $\boldsymbol{d}_n \in \mathbb{C}^{M\times 1}$, with $n \in \mathcal{N} \triangleq \{0, 1, \ldots, N-1\}$. Each precoded vector $\boldsymbol{d}_n$ passes through a redundancy insertion block generating the vector $\boldsymbol{x}_n \in \mathbb{C}^{P\times 1}$, in which $P \triangleq M + R$, with R denoting the number of redundant elements added as guard interval in the form of zero padding (ZP).

The continuous-time signal $\tilde{x}_n(t)$ that feeds the RF chain of the n^{th} antenna element is the output of a digital-to-analog converter (DAC) with sampling time T_s; thus, by defining the index set $\mathcal{P} \triangleq \{0, 1, \ldots, P-1\}$, one has

$$\tilde{x}_n(t) \triangleq \sum_{p\in\mathcal{P}} x_n[p] \cdot f(t - pT_\text{s}) = (x_n * f)(t), \qquad (1)$$

where $f(t)$ denotes the transmitting pulse (e.g., a square-root raised cosine — SRRC) and $x_n(t) \triangleq \sum_{p\in\mathcal{P}} x_n[p] \cdot \delta(t - pT_\text{s})$.

The energy required to transmit the precoded signals is

$$E \triangleq \sum_{n\in\mathcal{N}} \int_{-\infty}^{\infty} \frac{|\tilde{x}_n(t)|^2}{Z_0} \mathrm{d}t = \frac{1}{Z_0} \sum_{n\in\mathcal{N}} \boldsymbol{x}_n^{\text{H}} \boldsymbol{C}_f \boldsymbol{x}_n\,, \qquad (2)$$

in which $Z_0 > 0$ denotes the antenna impedance, $|\tilde{x}_n(t)|^2/Z_0$ is the instantaneous power, and $[\boldsymbol{C}_f]_{p_1,p_2} \triangleq (f * f)((p_1 - p_2)T_\text{s})$, for all $p_1, p_2 \in \mathcal{P}$.

Assume a quasi-static flat fading channel during the transmission of one block of signals, and let $\tilde{h}_{k,n}$ denote the attenuation of the base-band physical link between the n^{th} transmitting antenna and the k^{th} user terminal. The base-band signal received by the k^{th} user is $\tilde{y}_k(t) \triangleq \sum_{n\in\mathcal{N}} \tilde{h}_{k,n} \cdot \tilde{x}_n(t) + \tilde{v}_k(t)$, in which $\tilde{v}_k(t)$ is an additive noise signal.

Consider the receiver structure of the k^{th} user depicted in Fig. 2. The signal at the output of the receiving filter $g(t)$ is

$$y_k(t) \triangleq \sum_{n\in\mathcal{N}} \sum_{p\in\mathcal{P}} x_n[p] \cdot h_{k,n}(t - pT_\text{s}) + v_k(t)\,, \qquad (3)$$

in which $v_k(t) \triangleq (g * \tilde{v}_k)(t)$ and $h_{k,n}(t) \triangleq \tilde{h}_{k,n} \cdot (g * f)(t)$ is the equivalent base-band channel model. After sampling the signal $y_k(t)$, the resulting samples are collected in the vector $\boldsymbol{y}_k \in \mathbb{C}^{P\times 1}$ and then processed via a redundancy removal step before the actual symbol detection.

Usually, $(f * g)(t)$ is a T-Nyquist filter with roll-off factor $\rho \in [0, 1]$, so that no ISI is induced as long as: (i) $T_\text{s} = T$; (ii) the received signal employs the same sampling time T_s; and (iii) there is no time offset. Indeed, $(f * g)(pT) \propto \delta[p - p_0]$, where p_0 is a discrete delay; this means the transmitting/receiving filters spread the signal in time without inducing interference among the samples spaced apart at multiples of T. Next section addresses the case in which the transmission of signals are accelerated by using a sampling time $T_\text{s} < T$.

3. FASTER-THAN-NYQUIST SIGNALING

When $T_\text{s} = \alpha T$, with $\alpha \in (0, 1)$, the transmissions of samples are accelerated using an FTN signaling [14]. In this case, the equivalent channel $h_{k,n}(t)$ accounts for the ISI induced by the fact that the Nyquist pulse assumption is no longer valid, which might impact the parameters' choice of the system, such as the guard-interval length $R^{(\alpha)}$ defined in Section 2 — now with the explicit dependency on the factor α.

On the one hand, α should be made small to accelerate as much as possible the transmissions aiming to achieve higher data rates. On the other hand, $\alpha \leq 1$ should be made large to reduce the harmful ISI effects over the transmissions; notice also that, when there is significant ISI, bandwidth resources could also be spent in the transmission of redundant elements to cope with the underlying IBI, thus decreasing the spectral efficiency [27]. Hence, it is not straightforward to guarantee that, by decreasing α, one has spectral efficiency gains for the system model in Section 2; nor is clear to which extent α can be decreased without significantly harming the transmission performance.

To investigate these aspects further, assume that $\nu_{\max}^{(\alpha)}$ denotes the order of the finite-duration discrete-time model of the MISO channel for a sampling time $T_\text{s} = \alpha T$. For another sampling time $T_\text{s}' = \alpha' T$, with $\alpha' \in (0, 1]$, one has $\nu_{\max}^{(\alpha')} \approx \left(\frac{\alpha}{\alpha'}\right) \cdot \nu_{\max}^{(\alpha)}$. As the number of redundant elements $R^{(\alpha)}$ is usually proportional to $\nu_{\max}^{(\alpha)}$ [23, 27], let us assume that $R^{(\alpha')} = \left\lfloor \frac{\alpha}{\alpha'} \right\rfloor \cdot R^{(\alpha)}$. Thus, consider the following definition.

Definition 1. The *error-free spectral efficiency* is

$$\mathrm{SE}_0(\alpha) \triangleq \frac{M}{M + R^{(\alpha)}} \cdot \frac{1}{\alpha} \cdot \frac{b \cdot r_\text{c}}{2(1+\rho)} \quad [\text{bit/s/Hz}], \qquad (4)$$

in which b is the number of bits per constellation symbol, r_c is the channel coding rate, and $\rho \in [0, 1]$ is the roll-off factor.

With this definition, one has the following result.

Proposition 1. $\mathrm{SE}_0(\alpha)$ *is a decreasing function of* $\alpha \in (0, 1]$.

Proof. For fixed b, r_c, ρ, as $\mathrm{SE}_0(\alpha) \propto \frac{M}{M+R^{(\alpha)}} \frac{1}{\alpha}$ and

$$\begin{aligned} \frac{M}{M + R^{(\alpha')}} \frac{1}{\alpha'} &= \frac{M}{\alpha' M + \alpha' \left\lfloor \frac{\alpha}{\alpha'} \right\rfloor R^{(\alpha)}} \\ &\geq \frac{M}{\left(\frac{\alpha'}{\alpha}\right) M + R^{(\alpha)}} \frac{1}{\alpha} \\ &= \frac{M}{M + R^{(\alpha)}} \frac{1}{\alpha} \left(\frac{1}{1 - \frac{\left[1 - \left(\frac{\alpha'}{\alpha}\right)\right] M}{M + R^{(\alpha)}}} \right), \end{aligned} \qquad (5)$$

then, when $\alpha' < \alpha$, one has $\frac{\left[1-\left(\frac{\alpha'}{\alpha}\right)\right] M}{M+R^{(\alpha)}} < 1$, thus implying that $\frac{M}{M+R^{(\alpha')}} \frac{1}{\alpha'} > \frac{M}{M+R^{(\alpha)}} \frac{1}{\alpha} \Leftrightarrow \mathrm{SE}_0(\alpha') > \mathrm{SE}_0(\alpha)$. □

Remark 1. In fact, from the proof of Proposition 1, one can be more precise and state that the relative gain in the error-free spectral efficiency that one can get from decreasing α to α' is

$$\frac{\mathrm{SE}_0(\alpha') - \mathrm{SE}_0(\alpha)}{\mathrm{SE}_0(\alpha)} \geq \left[1 - \left(\frac{\alpha'}{\alpha}\right)\right] \frac{M}{M + R^{(\alpha)}} \,. \tag{6}$$

These results suggest that one should decrease T_s as much as possible; yet, when doing so, the channel taps $h_{k,n}[p]$ also change (even if the physical link is kept the same). This eventually means one cannot discard the possibility of having an equivalent channel more favorable to the transmission (performance-wise, so to speak) when using a larger T_s, which eventually might impact the *effective* spectral efficiency — the one considering transmission errors. Besides, there is a lower-bound, $\alpha_{\min} \in (0, 1]$, for α to guarantee information losslessness in the following sense.

Definition 2. The pair $(f(t), T_\mathrm{s})$ yields an *information-losslessness transmission* if, given $\tilde{x}_n(t)$ in (1), there exists a receiving filter $g(t)$ such that $\hat{x}_n[p] \triangleq \hat{x}_n(pT_\mathrm{s}) = x_n[p], \forall p \in \mathcal{P}$, with $\hat{x}_n(t) \triangleq (\tilde{x}_n * g)(t)$.

The following lemma characterizes the transmitting filters that enable information-losslessness transmissions.

Lemma 1. The information-losslessness condition in Definition 2 is met if and only if $\sum_{q\in\mathbb{Z}} \left|F\left(\mathrm{j}\frac{(\omega+2\pi q)}{T_\mathrm{s}}\right)\right|^2 > 0, \forall \omega \in \mathbb{R}$.

Proof. See Lemmas 5.1 and 5.2 in [28]. □

Assuming a square-root T-Nyquist transmitting filter with roll-off factor $\rho \in [0, 1]$, one has the following result.

Proposition 2. $\alpha_{\min} = \frac{1}{1+\rho}$.

Proof. From Lemma 1, we note that the necessary and sufficient condition for information losslessness can be rewritten as $B^2(\mathrm{j}\omega) > 0, \forall \omega \in \mathbb{R}$, for $B^2(\mathrm{j}\omega) \triangleq \sum_{q\in\mathbb{Z}} \left|F\left(\mathrm{j}\frac{(\omega T+2\pi q)}{T_\mathrm{s}}\right)\right|^2$. As $f(t)$ is a square-root T-Nyquist filter with roll-off ρ, then $F\left(\mathrm{j}\frac{(\omega T+2\pi q)}{T_\mathrm{s}}\right) = F\left(\frac{\mathrm{j}}{\alpha}\frac{(\omega T+2\pi q)}{T}\right) = 0$ for $\omega \notin \left(-\frac{\alpha(1+\rho)\pi}{T} - \frac{2\pi q}{T}, \frac{\alpha(1+\rho)\pi}{T} - \frac{2\pi q}{T}\right)$. In this case, $B^2(\mathrm{j}\omega) > 0, \forall \omega \in \mathbb{R}$ iff the intersection of the adjacent supports of $F\left(\mathrm{j}\frac{(\omega T+2\pi q)}{T_\mathrm{s}}\right)$ and $F\left(\mathrm{j}\frac{(\omega T+2\pi (q+1))}{T_\mathrm{s}}\right)$ is nonempty; iff: $-\frac{\alpha(1+\rho)\pi}{T} - \frac{2\pi q}{T} \leq \frac{\alpha(1+\rho)\pi}{T} - \frac{2\pi(q+1)}{T} \Leftrightarrow \alpha\cdot(1+\rho) \geq 1$. □

Next section describes how the redundancy addition/removal can deal with IBI effects arising from using $\alpha < 1$.

4. REDUNDANT BLOCK-BASED TRANSMISSIONS

For FTN sequential transmissions, the l^{th} received block after sampling, synchronization, and buffering can be written as (see also (3))

$$\boldsymbol{y}_k[l] = \sum_{n\in\mathcal{N}} \Big(\boldsymbol{H}_{\mathrm{ISI}_{k,n}} \boldsymbol{x}_n[l] + \boldsymbol{H}^{(\mathrm{b})}_{\mathrm{IBI}_{k,n}} \boldsymbol{x}_n[l-1] + \boldsymbol{H}^{(\mathrm{f})}_{\mathrm{IBI}_{k,n}} \boldsymbol{x}_n[l+1] \Big) + \boldsymbol{v}_k[l] \,, \tag{7}$$

in which the ISI and backward/forward IBI matrices are $P \times P$ Toeplitz matrices with first columns

$$\boldsymbol{H}_{\mathrm{ISI}_{k,n}}(:,1) \triangleq \Big[h_{k,n}[0] \quad \cdots \quad h_{k,n}[\nu^{(\alpha)}_{\max}/2] \quad 0 \quad \cdots \quad 0\Big]^{\mathrm{T}},$$
$$\boldsymbol{H}^{(\mathrm{b})}_{\mathrm{IBI}_{k,n}}(:,1) \triangleq \boldsymbol{0}_{P\times 1},$$
$$\boldsymbol{H}^{(\mathrm{f})}_{\mathrm{IBI}_{k,n}}(:,1) \triangleq \Big[0 \quad \cdots \quad 0 \quad h_{k,n}[-\nu^{(\alpha)}_{\max}/2] \quad \cdots \quad h_{k,n}[-1]\Big]^{\mathrm{T}},$$

and with first rows

$$\boldsymbol{H}_{\mathrm{ISI}_{k,n}}(1,:) \triangleq \Big[h_{k,n}[0] \quad \cdots \quad h_{k,n}[-\nu^{(\alpha)}_{\max}/2] \quad 0 \quad \cdots \quad 0\Big],$$
$$\boldsymbol{H}^{(\mathrm{b})}_{\mathrm{IBI}_{k,n}}(1,:) \triangleq \Big[0 \quad \cdots \quad 0 \quad h_{k,n}[\nu^{(\alpha)}_{\max}/2] \quad \cdots \quad h_{k,n}[1]\Big],$$
$$\boldsymbol{H}^{(\mathrm{f})}_{\mathrm{IBI}_{k,n}}(1,:) \triangleq \boldsymbol{0}_{1\times P},$$

in which $\nu^{(\alpha)}_{\max} < 2M$ is assumed to be an even integer w.l.o.g.

In order to deal with the IBI possibly harmful effects, we propose the use of redundant zero-padding zero-jamming (ZP-ZJ) transceivers [23, 24, 25, 26, 27] with an adjustable amount of redundant elements which are added and removed through the multiplication by the matrices (see Figs. 1 and 2)

$$\boldsymbol{A} \triangleq \begin{bmatrix} \boldsymbol{0}_{\frac{R(\alpha)}{2}\times M} \\ \boldsymbol{I}_M \\ \boldsymbol{0}_{\frac{R(\alpha)}{2}\times M} \end{bmatrix}, \; \boldsymbol{R} \triangleq \Big[\boldsymbol{0}_{M\times\frac{R(\alpha)}{2}} \quad \boldsymbol{I}_M \quad \boldsymbol{0}_{M\times\frac{R(\alpha)}{2}}\Big], \tag{8}$$

where $R^{(\alpha)}$ is constrained to be an even integer.

Given the pair $(\boldsymbol{A}, \boldsymbol{R})$ in (8), it is straightforward to verify that the following result holds.

Proposition 3. *The minimum guard-interval length that enables IBI-free transmissions is* $R^{(\alpha)}_{\text{IBI-free}} \triangleq 2 \cdot \left\lceil \frac{\nu^{(\alpha)}_{\max}}{4} \right\rceil$.

Indeed, when using $R^{(\alpha)} \geq R^{(\alpha)}_{\text{IBI-free}}$ redundant elements, one has $\boldsymbol{R}\boldsymbol{H}^{(\mathrm{b})}_{\mathrm{IBI}_{k,n}}\boldsymbol{A} = \boldsymbol{R}\boldsymbol{H}^{(\mathrm{f})}_{\mathrm{IBI}_{k,n}}\boldsymbol{A} = \boldsymbol{0}_{M\times M}$. We propose employing an adjustable reduced amount of redundant elements

$$R^{(\alpha)} \in \mathcal{R}^{(\alpha)} \triangleq \Big\{2r \,|\, r \in \mathbb{Z}_+ \text{ and } 0 \leq 2r \leq R^{(\alpha)}_{\text{IBI-free}}\Big\}, \tag{9}$$

which allows us to control the degree of remaining IBI given by $\sum_{n\in\mathcal{N}} \boldsymbol{R}\boldsymbol{H}^{(\mathrm{b})}_{\mathrm{IBI}_{k,n}}\boldsymbol{A}\boldsymbol{d}_n[l-1] + \boldsymbol{R}\boldsymbol{H}^{(\mathrm{f})}_{\mathrm{IBI}_{k,n}}\boldsymbol{A}\boldsymbol{d}_n[l+1]$.

5. SPATIOTEMPORAL SYMBOL-LEVEL PRECODING

Considering the system model described in Section 2 and the block-based transceiver proposed in Section 4, the reconstructed signals of all users can be written as

$$\hat{\boldsymbol{s}}[l] = \boldsymbol{H}_{\mathrm{ISI}}\boldsymbol{d}[l] + \boldsymbol{H}_{\mathrm{IBI}}\boldsymbol{d}[l-1] + \boldsymbol{z'}[l] \,, \tag{10}$$

which corresponds to the vector stacking of the signals $\hat{\boldsymbol{s}}_k[l]$, with $\boldsymbol{H}_{\mathrm{ISI}}$ comprising the matrices $\boldsymbol{R}\boldsymbol{H}_{\mathrm{ISI}_{k,n}}\boldsymbol{A}$, for $(k,n) \in \mathcal{K}\times\mathcal{N}$, that model the transfer from $\hat{\boldsymbol{d}}_n[l]$ to $\hat{\boldsymbol{s}}_k[l]$, and $\boldsymbol{H}_{\mathrm{IBI}}$ comprising the matrices $\boldsymbol{R}\boldsymbol{H}^{(\mathrm{b})}_{\mathrm{IBI}_{k,n}}\boldsymbol{A}$, for $(k,n) \in \mathcal{K}\times\mathcal{N}$, that model the transfer from $\hat{\boldsymbol{d}}_n[l-1]$ (*known* at instant l) to $\hat{\boldsymbol{s}}_k[l]$, whereas $\boldsymbol{z'}[l]$ denotes the interference-plus-noise component due to the remaining forward IBI components $\boldsymbol{R}\boldsymbol{H}^{(\mathrm{f})}_{\mathrm{IBI}_{k,n}}\boldsymbol{A}\boldsymbol{d}_n[l+1]$ (*unknown* at instant l) and the noise $\boldsymbol{z}_k[l]$.

We propose using a spatiotemporal SLP scheme accounting for MUI and FTN-induced interference — in the form of both ISI and IBI. The idea is to exploit the interference in both spatial and temporal domains in a constructive manner. The backward IBI could help constructively in the transmission, but the remaining forward IBI tends to degrade the system performance, suggesting a trade-off between those effects. Given the energy E in (2), with $\boldsymbol{x}_n[l] = \boldsymbol{A}\boldsymbol{d}_n[l]$, the proposed SLP *convex* optimization problem is

$$\begin{aligned} \underset{\boldsymbol{d}[l]\in\mathbb{C}^{NM\times 1}}{\text{minimize}} \quad & E[l] \\ \text{subject to} \quad & \boldsymbol{H}_{\mathrm{ISI}}\boldsymbol{d}[l] + \boldsymbol{H}_{\mathrm{IBI}}\boldsymbol{d}[l-1] \succeq \boldsymbol{q} \odot \boldsymbol{s}[l] \,, \end{aligned} \tag{11}$$

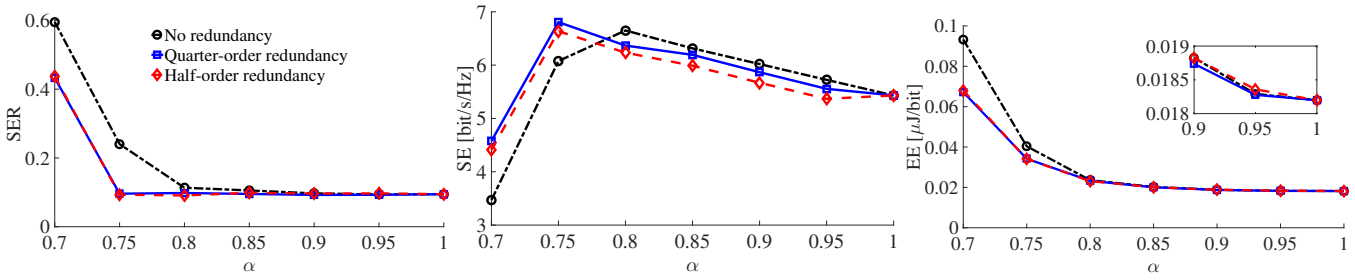

(a) Average symbol-error rate (SER). (b) Sum effective spectral efficiency (SE). (c) Overall energy efficiency (EE).

Fig. 3. Performance of the proposed spatiotemporal SLPs for different FoMs as functions of the acceleration factor α (*Experiment 2*).

in which $\boldsymbol{s}[l] \in \mathbb{C}^{KM\times 1}$ contains the actual transmitted symbols, $\boldsymbol{q} \in \mathbb{C}^{KM\times 1}$ collects quality-of-service-related parameters, such as target signal-to-interference-plus-noise ratio (SINR) and noise variance, and $\odot$ denotes point-wise product between vectors. The operator $\trianglerighteq$ can be defined in different ways depending on the specific constellation points $\boldsymbol{s}[l]$; in all cases, the operator $\trianglerighteq$ defines a convex constraint set (polyhedron) — please refer to [5, 6, 7, 8, 10, 20, 21] for further specific details. Low-complexity techniques can be used to tackle the problem in (11) — see [29] and references therein.

6. NUMERICAL RESULTS

The performance of the proposed precoders is assessed via three experiments. The numbers of subcarriers, transmitting antennas, and users are respectively fixed at $M = 64$, $N = 4$, and $K = 4$. The transmitting/receiving filters are T-SRRC pulses for a fixed Nyquist period $T = 100$ ns. The antenna impedance in (2) is $Z_0 = 50\,\Omega$.

The figures of merit (FoMs) are: (i) average symbol error rate, $\mathrm{SER} \triangleq \frac{1}{K}\sum_{k\in\mathcal{K}} \mathrm{SER}^{(k)}$, (ii) sum effective spectral efficiency, $\mathrm{SE} \triangleq K \cdot \mathrm{SE}_0 \cdot (1 - \mathrm{SER})$, and (iii) overall energy efficiency, $\mathrm{EE} \triangleq \frac{\text{average power}}{\mathrm{SE}}$, with 'average power' computed as the total analog power feeding the antennas averaged over the interval $P \cdot T_\mathrm{s}$.[1]

Experiment 1: We showcase the advantages of using FTN from the energy-efficiency viewpoint considering two different ways of doubling the error-free spectral efficiency in Definition 1, to wit: doubling the constellation size b and halving the factor α. From Proposition 2, we set $\rho = 1$ to attain $\alpha = 0.5$. A non-redundant precoder ($R^{(\alpha)} = 0$) is employed. A 16-QAM transmission with $\alpha = 1$ yields $\mathrm{EE} \approx 13\ \mu\mathrm{J/bit}$, whereas an FTN 4-QAM transmission with $\alpha = 0.5$ yields $\mathrm{EE} \approx 6\ \mu\mathrm{J/bit}$, where both transmissions operate at the same $\mathrm{SER} \approx 9.5\%$ and $\mathrm{SE} \approx 3.6$ bit/s/Hz.

Experiment 2: We study the performance of three precoders with respect to different factors α for a 16-QAM transmission, a roll-off factor $\rho = \frac{1}{3}$, and a quality of service $\boldsymbol{q} = \sqrt{\gamma}\mathbf{1}_{KM\times 1}$, where the target SINR γ corresponds to 12 dB. The guard-interval length is chosen as: (i) $R^{(\alpha)} = 0$, called 'no redundancy' [20, 21], (ii) $R^{(\alpha)} \approx \frac{\nu_{\max}^{(\alpha)}}{4}$, called 'quarter-order redundancy', and (iii) $R^{(\alpha)} \approx \frac{\nu_{\max}^{(\alpha)}}{2}$, called 'half-order redundancy'.[2] Fig. 3 depicts the results. Note that the break point for the SER performance in Fig. 3(a) appears at $\alpha = \frac{1}{1+\rho}$ for the redundant systems. In addition, Fig. 3(b) lets clear that the non-redundant precoder performs well in terms of effective spectral efficiency for moderate acceleration factors down to $\alpha = 0.80$, whereas the redundant precoders are the best under severe ISI (at $\alpha = 0.75$). Notice that the gain in SE comes at the cost of spending more energy per bit when compared to non-FTN transmissions ($\alpha = 1$), as shown in Fig. 3(c).

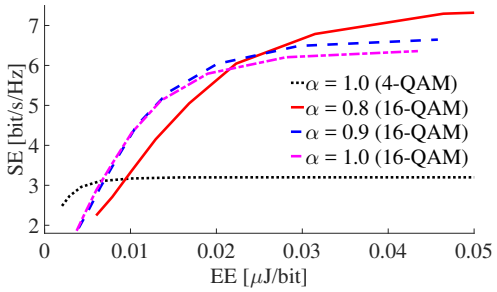

Fig. 4. SE $\times$ EE for different acceleration factors and constellation sizes considering a quarter-order redundant precoder (*Experiment 3*).

Experiment 3: We study the SE vs. EE behavior by varying the target SINR (from 0 to 16 dB) comprising vector $\boldsymbol{q}$ for the quarter-order redundant precoder, with a roll-off factor $\rho = \frac{1}{4}$. The results are shown in Fig. 4. One can clearly see that, depending on the operating point on the SE $\times$ EE plane, it might be better to use one precoder over the other; for instance, at $\mathrm{EE} = 0.04\ \mu\mathrm{J/bit}$, 16-QAM with $\alpha = 0.8$ is the best choice, whereas at $\mathrm{EE} = 0.01\ \mu\mathrm{J/bit}$, the non-FTN 16-QAM system could be picked up.

7. CONCLUDING REMARKS

In this paper, we have addressed the problem of jointly handling multi-user and intersymbol interference in multi-antenna downlink transmissions relying on FTN signaling. More specifically, block-based spatiotemporal symbol-level precoding schemes have been proposed, where the introduction of redundancy achieves a trade-off between constructive/destructive MUI and IBI effects at the user terminals. Numerical results have shown that the proposed schemes can outperform Nyquist-based transmissions in terms of spectral efficiency, with limited loss in energy efficiency, as long as the considered acceleration factor is not lower than a certain value (which, in turn, is related to the roll-off factor of the transmitting filter). Further, numerical results have highlighted how the introduction of redundancy in the block-based transmissions enhances the system acceleration (lower acceleration factors), since the introduced interference (in particular the IBI) is handled more effectively as compared to the non-redundant solution. Future works include extending the proposals to multicarrier systems with frequency packing for frequency-selective channels.

[1] Unlike [20, 21], here we consider the actual analog power including the cross-power terms resulting from the sequential transmission.

[2] We actually employed the smallest even integer larger than or equal to either $\nu_{\max}^{(\alpha)}/4$ (quarter-order redundancy) or $\nu_{\max}^{(\alpha)}/2$ (half-order redundancy).

8. REFERENCES

[1] C. Masouros and E. Alsusa, "Dynamic linear precoding for the exploitation of known interference in MIMO broadcast systems," *IEEE Trans. Wireless Commun.*, vol. 8, no. 3, pp. 1396–1404, Mar 2009.

[2] C. Masouros, "Correlation rotation linear precoding for MIMO broadcast communications," *IEEE Trans. Signal Process.*, vol. 59, no. 1, pp. 252–262, Jan 2011.

[3] M. Alodeh, S. Chatzinotas, and B. Ottersten, "Constructive multiuser interference in symbol level precoding for the MISO downlink channel," *IEEE Trans. Signal Process.*, vol. 63, no. 9, pp. 2239–2252, May 2015.

[4] C. Masouros and G. Zheng, "Exploiting known interference as green signal power for downlink beamforming optimization," *IEEE Trans. Signal Process.*, vol. 63, no. 14, pp. 3628–3640, July 2015.

[5] M. Alodeh, S. Chatzinotas, and B. Ottersten, "Energy-efficient symbol-level precoding in multiuser MISO based on relaxed detection region," *IEEE Trans. Wireless Commun.*, vol. 15, no. 5, pp. 3755–3767, May 2016.

[6] M. Alodeh, S. Chatzinotas, and B. Ottersten, "Symbol-level multiuser MISO precoding for multi-level adaptive modulation," *IEEE Trans. Wireless Commun.*, vol. 16, no. 8, pp. 5511–5524, Aug 2017.

[7] D. Spano, M. Alodeh, S. Chatzinotas, and B. Ottersten, "Symbol-level precoding for the nonlinear multiuser MISO downlink channel," *IEEE Trans. Signal Process.*, vol. 66, no. 5, pp. 1331–1345, Mar 2018.

[8] A. Haqiqatnejad, F. Kayhan, and B. Ottersten, "Constructive interference for generic constellations," *IEEE Signal Process. Lett.*, vol. 25, no. 4, pp. 586–590, Apr 2018.

[9] Y. Choi, J. Lee, M. Rim, and C. G. Kang, "Constructive interference optimization for data-aided precoding in multi-user MISO systems," *IEEE Trans. Wireless Commun.*, vol. 18, no. 2, pp. 1128–1141, Feb 2019.

[10] M. Alodeh, D. Spano, A. Kalantari, C. G. Tsinos, D. Christopoulos, S. Chatzinotas, and B. Ottersten, "Symbol-level and multicast precoding for multiuser multiantenna downlink: A state-of-the-art, classification, and challenges," *IEEE Commun. Surveys Tuts.*, vol. 20, no. 3, pp. 1733–1757, third-quarter 2018.

[11] J. E. Mazo, "Faster-than-Nyquist signaling," *The Bell Syst. Tech. J.*, vol. 54, no. 8, pp. 1451–1462, Oct 1975.

[12] A. D. Liveris and C. N. Georghiades, "Exploiting faster-than-Nyquist signaling," *IEEE Trans. Commun.*, vol. 51, no. 9, pp. 1502–1511, Sep 2003.

[13] F. Rusek and J. B. Anderson, "The two dimensional Mazo limit," in *Proc. IEEE Int. Symp. Inf. Theory (ISIT)*, Sep 2005, pp. 970–974.

[14] J. B. Anderson, F. Rusek, and V. wall, "Faster-than-Nyquist signaling," *Proc. IEEE*, vol. 101, no. 8, pp. 1817–1830, Aug 2013.

[15] Y. J. D. Kim, J. Bajcsy, and D. Vargas, "Faster-than-Nyquist broadcasting in Gaussian channels: Achievable rate regions and coding," *IEEE Trans. Commun.*, vol. 64, no. 3, pp. 1016–1030, Mar 2016.

[16] M. Alodeh, D. Spano, S. Chatzinotas, and B. Ottersten, "Faster-than-Nyquist spatiotemporal symbol-level precoding in the downlink of multiuser MISO channels," in *Proc. IEEE Int. Conf. Acoust., Speech and Signal Process. (ICASSP)*, Mar 2017, pp. 3779–3783.

[17] T. Xu, C. Masouros, and I. Darwazeh, "Waveform and space precoding for next generation downlink narrowband IoT," *IEEE Internet of Things J.*, vol. 6, no. 3, pp. 5097–5107, June 2019.

[18] Q. Li, F. Gong, P. Song, and S. Zhai, "Pre-equalized interference cancellation for faster-than-Nyquist signaling," *IEEE Access*, vol. 7, pp. 77868–77876, June 2019.

[19] M. Jana, L. Lampe, and J. Mitra, "Precoded time-frequency-packed multicarrier faster-than-Nyquist transmission," in *Proc. IEEE Int. Workshop Signal Process. Advances Wireless Commun. (SPAWC)*, July 2019, pp. 1–5.

[20] D. Spano, S. Chatzinotas, and B. Ottersten, "Sequential spatia-temporal symbol-level precoding enabling faster-than-Nyquist signaling for multi-user MISO systems," in *Proc. European Signal Process. Conf. (EUSIPCO)*, Sep 2018, pp. 827–831.

[21] D. Spano, M. Alodeh, S. Chatzinotas, and B. Ottersten, "Faster-than-Nyquist signaling through spatio-temporal symbol-level precoding for the multiuser MISO downlink channel," *IEEE Trans. Wireless Commun.*, vol. 17, no. 9, pp. 5915–5928, Sep 2018.

[22] A. Scaglione, G. B. Giannakis, and S. Barbarossa, "Redundant filterbank precoders and equalizers. I. unification and optimal designs," *IEEE Trans. Signal Process.*, vol. 47, no. 7, pp. 1988–2006, July 1999.

[23] Y.-P. Lin and S.-M. Phoong, "Minimum redundancy for ISI free FIR filterbank transceivers," *IEEE Trans. Signal Process.*, vol. 50, no. 4, pp. 842–853, Apr 2002.

[24] W. A. Martins and P. S. R. Diniz, "Block-based transceivers with minimum redundancy," *IEEE Trans. Signal Process.*, vol. 58, no. 3, pp. 1321–1333, Mar 2010.

[25] W. A. Martins and P. S. R. Diniz, "LTI transceivers with reduced redundancy," *IEEE Trans. Signal Process.*, vol. 60, no. 2, pp. 766–780, Feb 2012.

[26] W. A. Martins and P. S. R. Diniz, "DHT-based transceivers with reduced redundancy," *IEEE Trans. Signal Process.*, vol. 60, no. 11, pp. 6080–6085, Nov 2012.

[27] P. S. R. Diniz, W. A. Martins, and M. V. S. Lima, *Block Transceivers: OFDM and Beyond*, Morgan & Claypool, 2012.

[28] P. P. Vaidyanathan, S.-M. Phoong, and Y.-P. Lin, *Signal Processing and Optimization for Transceiver Systems*, Cambridge University Press, 2010.

[29] A. Haqiqatnejad, F. Kayhan, and B. Ottersten, "An approximate solution for symbol-level multiuser precoding using support recovery," in *Proc. IEEE Int. Workshop Signal Process. Advances Wireless Commun. (SPAWC)*, July 2019, pp. 1–5.